Force-Sensorless Position/Force Control Method for Continuous Shape-Grinding

○ 陳　光華 (福井大)　王　庚 (福井大)　見浪　護 (福井大)

Guanghua CHEN, Geng WANG Graduate school of engineering,
University of Fukui, 3-9-1, Bunkyo, Fukui, 910-8507, Japan
Mamoru MINAMI, University of Fukui, Bunkyo3-9-1, Fukui

Based on the analysis of the interaction between a manipulator's hand and a working object, a model representing the constraint dynamics of the robot is first discussed. The constraint forces are expressed by an algebraic function of states, input generalized forces, and constraint condition, and then direct position / force controller without force sensor is proposed based on the algebraic relation. To give the grinding system the ability to adapt to any object shape being changed by grinding, we added a function estimating the constraint condition in real time for the adaptive position / force control. Evaluations through simulations by fitting the changing constraint surface with spline functions, indicate that reliable position / force control and shape-grinding can be achieved by the proposed controller. Furthermore, experiment by using this proposed constraint condition estimating method has been done initially.

Keywords : direct position/force controller without force sensor, algebraic function, constraint condition estimating method

1 INTRODUCTION

Many researches have discussed on the force control of robots for contacting tasks. Most force control strategies are to use force sensors [1]-[5] to obtain force information, where the reliability and accuracy are limited since the work-sites of the robot are filled with noise and thermal disturbances. On top of this, force sensors could lead to the falling of the structure stiffness of manipulators, which is one of the most essential defects for manipulators executing grinding tasks. To solve these problems, some approaches using no force sensor have been presented [6]-[8]. To ensure the stabilities of the constrained motion, those force and position control methods have utilized Lyapunov's stability analysis under the inverse dynamic compensation [9]-[11]. Their force control strategies have been explained intelligibly in books and recently interaction control for six-degree-of-freedom tasks has been compiled.

However, insofar as we survey the controllers introduced in the books or published papers those papers don't base on the algebraic function of states and input generalized forces derived from the relation between the constraint condition and the equation of dynamics. So we discuss first a strategy for simultaneous control of the position and force without any force sensors, where the equation of dynamics in reference to the constrained force has been reformulated. The constrained force is derived from the equation of dynamics and the constrained equation as an explicit algebraic function of states and input generalized forces, which means force information can be obtained by calculation rather than by force sensing. Equation (1), which has been pointed out by Hemami in the analysis of biped walking robot, denotes also algebraic relation between the input torque $\boldsymbol{\tau}$ of the robot and exerting force to the working object F_n, when robot's end-effecter being in touch with a surface in 3-D space:

$$F_n = a(\boldsymbol{x}_1, \boldsymbol{x}_2) - \boldsymbol{A}(\boldsymbol{x}_1)\boldsymbol{\tau}, \tag{1}$$

where, $\boldsymbol{x}_1$ and $\boldsymbol{x}_2$ are state variables. $a(\boldsymbol{x}_1, \boldsymbol{x}_2)$ and $\boldsymbol{A}(\boldsymbol{x}_1)$ are scalar function and vector one defined in following section. This algebraic equation has been known, but it was the first time in robotics to be applied to the sensing function of exerting force by Peng [10]. There are controllers excluding any force feedback sensors but realizing simultaneous control of position and force in the constrained motions [1], [5], [7], [9].

A strategy to control force and position proposed in this paper is also based on (1). Contrarily to Peng's Method to use (1) as a force sensor, we used the equation for calculating $\boldsymbol{\tau}$ to achieve a desired exerting force F_{nd}. Actually, the strategy is based on two facts of (1) that have been ignored for a long time. The first fact is that the force transmission process is an immediately process being stated clearly by (1) providing that the manipulator's structure is rigid. Contrarily, the occurrence of velocity and position is a time-consuming process. By using this algebraic relation, it's possible to control the exerting force to the desired one without time lag. Another important fact is the input generalized forces have some redundancy against the constrained generalized forces in the constrained motion. Based on the above analysis, we had confirmed our force / position control method can realize the grinding task through real grinding robot.

The problem to be solved in our approach is that the mathematical expression of algebraic constraint condition should be defined in the controller instead of the merit of not using force sensor. Grinding task requires on-line estimation of changing constraint condition since the grinding is the action to change the con-

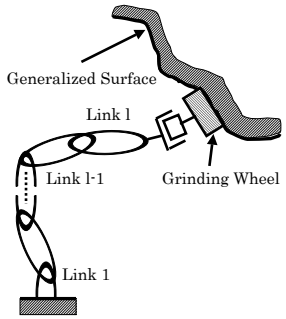

Fig. 1: A grinding robot

straint condition. In [4], we estimated the object's surface using the grinder as a touch sensor, updated the changing constraint condition in real time, and simulation results showed that spline function is best for on-line shape estimation. Based on the above preparation, we constructed a grinding robot to complete the grinding experiment by using this proposed constraint condition estimating method when the constraint surface is flat, the experiment results will be discussed at the end of this paper.

2 ANALYSIS OF GRINDING TASK

Generally speaking, the grinding power is related to the metal removal rate(weight of metal being removed within unit time), which is determined by the depth of cut, the width of cut, the linear velocity of the grinding wheel, the feed rate and so on. There are many empirical formulae available for the determination of grinding power, and the desired force trajectory can then be planned according to the power. The normal grinding force F_n is exerted in the perpendicular direction of the surface. It is a significant factor that affects ground accuracy and surface roughness of workpiece. The value F_n is also related to the grinding power or directly to the tangential grinding force as

$$F_t = \mathrm{K_t} F_n, \tag{2}$$

where, $\mathrm{K_t}$ is an empirical coefficient, F_t is the tangential grinding force.

The axial grinding force F_s is proportional with the feed rate, and is much smaller than the former force.

Equation (2) is based on the situation that position of the grinding cutter is controlled like currently used machining center. But when a robot is used for the grinding task, the exerting force to the object and the position of the grinding cutter should be controlled simultaneously. And the F_n is generally determined by the constrained situation.

For grinding task, the normal force and tangential velocity are the most important two factors. To improve grinding quality, it is usually desired that the normal force is constant while the velocity is also constant in the middle term of a grinding stroke.

Grinding is a kind of precision machining method and the working condition is hard for a robot to do it precisely to a certain extent because of the rather large contacting forces. Hence, force control is necessary besides position control. Usually, force sensor is an essential element to control the force. However, the sensors pose many problems as the above-mentioned. If possible, sensing without sensors is much better for the merit of that there is no difficulty on the design and no cost. The following will present how to obtain force information by calculating rather than by using force sensors.

3 MODELING

3.1 Constrained dynamical systems

Hemami and Wyman have addressed the issue of control of a moving robot according to constraint condition and examined the problem of the control of the biped locomotion constrained in the frontal plane. Their purpose was to control the position coordinates of the biped locomotion rather than generalized forces included in constrained dynamical equation. And the constrained force is used as a determining condition to change the dynamic model from constrained motion to free motion of the legs. In this paper, the grinding manipulator shown in Fig. 1, whose end-point is in contact with the constrained surface, is modelled as following (3) with Lagrangian equations of motion in term of the constraint forces, refering to what Hemami and Arimoto[7] have done:

$$\frac{d}{dt}\left(\frac{\partial L}{\partial \dot{\boldsymbol{q}}}\right) - \left(\frac{\partial L}{\partial \boldsymbol{q}}\right) = \boldsymbol{\tau} + \boldsymbol{J_c}^T(\boldsymbol{q}) F_n - \boldsymbol{J_r}^T(\boldsymbol{q}) F_t, \tag{3}$$

where, L is the Lagrangian function, V is potential function, $\boldsymbol{q}$ is $l(\geq 2)$ generalized coordinates, $\boldsymbol{\tau}$ is l inputs. $\boldsymbol{J_c}$ and $\boldsymbol{J_r}$ satisfy,

$$\boldsymbol{J_c} = \frac{\partial C}{\partial \boldsymbol{q}} / \parallel \frac{\partial C}{\partial \boldsymbol{r}} \parallel = \frac{\partial C}{\partial \boldsymbol{r}} \, \tilde{\boldsymbol{J}}_r \, / \parallel \frac{\partial C}{\partial \boldsymbol{r}} \parallel,$$

$$\tilde{\boldsymbol{J}}_r = \frac{\partial \boldsymbol{r}}{\partial \boldsymbol{q}}, \qquad \boldsymbol{J}_r^T = \tilde{\boldsymbol{J}}_r^{\,T} \, \dot{\boldsymbol{r}} / \parallel \dot{\boldsymbol{r}} \parallel,$$

$\boldsymbol{r}$ is the l position vector of the hand and can be expressed as a kinematic equation ,

$$\boldsymbol{r} = \boldsymbol{r}(\boldsymbol{q}).$$

The discussing robot system does not have kinematical redundancy. C is a scalar function of constraint, and expressed as an equation of constraint

$$C(\boldsymbol{r}(\boldsymbol{q})) = 0, \tag{4}$$

F_n is the constrained force associated with C and F_t is the tangential disturbance force.

Equation (3) can be extended to

$$\boldsymbol{M}(\boldsymbol{q})\ddot{\boldsymbol{q}} + \boldsymbol{H}(\boldsymbol{q}, \dot{\boldsymbol{q}}) + \boldsymbol{G}(\boldsymbol{q})$$

$$= \boldsymbol{\tau} + \boldsymbol{J}_c^T(\boldsymbol{q}) F_n - \boldsymbol{J}_r^T(\boldsymbol{q}) F_t, \tag{5}$$

where $\boldsymbol{M}$ is an $l \times l$ matrix, $\boldsymbol{H}$ and $\boldsymbol{G}$ are l vectors. The state variable $\boldsymbol{x}$ is constructed by adjoining $\boldsymbol{q}$ and $\dot{\boldsymbol{q}}$:

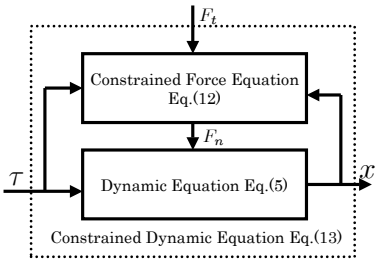

Fig. 2: Model of Constrained Dynamic System

$\boldsymbol{x} = (\boldsymbol{x}_1^T, \boldsymbol{x}_2^T)^T = (\boldsymbol{q}^T, \dot{\boldsymbol{q}}^T)^T$. The state-space equation of the system are

$$\begin{aligned} \dot{\boldsymbol{x}}_1 &= \boldsymbol{x}_2, \\ \dot{\boldsymbol{x}}_2 &= -\boldsymbol{M}^{-1}(\boldsymbol{H}(\boldsymbol{x}_1, \boldsymbol{x}_2) + \boldsymbol{G}(\boldsymbol{x}_1)) \\ &\quad +\boldsymbol{M}^{-1}(\boldsymbol{\tau} + \boldsymbol{J}_c^T(\boldsymbol{x}_1)F_n - \boldsymbol{J}_r^T\boldsymbol{x}_1)F_t), \end{aligned} \tag{6}$$

or in the compact form

$$\dot{\boldsymbol{x}} = \boldsymbol{F}(\boldsymbol{x}, \boldsymbol{\tau}, F_n, F_t), \tag{7}$$

where the dimension of $\boldsymbol{x}$ is $n = 2l$. In order to control the system (7) with constraints (4) , it can be started firstly by differentiating the constraint equation (4) twice with respect to time and rewriting the result in terms of $\boldsymbol{x}$:

$$\boldsymbol{D}(\boldsymbol{x})\dot{\boldsymbol{x}} = 0, \tag{8}$$

where, $\boldsymbol{D}(\boldsymbol{x})$ is vector that the constrained motion of the system is orthogonal. Premultiplying (7) by $\boldsymbol{D}(\boldsymbol{x})$ according to (8), we can get

$$\boldsymbol{D}(\boldsymbol{x})\boldsymbol{F}(\boldsymbol{x}, \boldsymbol{\tau}, F_n, F_t) = 0. \tag{9}$$

This is a linear equation about the unknown constrained force F_n , combining the constrained equation and the equation of motion. (9) can be uniquely solved for F_n as a function of the state $\boldsymbol{x}$ and input $\boldsymbol{\tau}$,

$$\begin{aligned} &-[\frac{\partial}{\partial \boldsymbol{q}}(\frac{\partial C}{\partial \boldsymbol{q}})\dot{\boldsymbol{q}}]\dot{\boldsymbol{q}} + (\frac{\partial C}{\partial \boldsymbol{q}})\boldsymbol{M}^{-1}(\boldsymbol{H}(\boldsymbol{q}, \dot{\boldsymbol{q}}) + \boldsymbol{G}(\boldsymbol{q}) + \boldsymbol{J_r}^T F_t) \\ &-(\frac{\partial C}{\partial \boldsymbol{q}})\boldsymbol{M}^{-1}\boldsymbol{\tau} = [(\frac{\partial C}{\partial \boldsymbol{q}})\boldsymbol{M}^{-1}(\frac{\partial C}{\partial \boldsymbol{q}})^T]F_n / \parallel \frac{\partial C}{\partial \boldsymbol{r}} \parallel, \end{aligned} \tag{10}$$

because the value of $(\frac{\partial C}{\partial \boldsymbol{q}})\boldsymbol{M}^{-1}(\frac{\partial C}{\partial \boldsymbol{q}})^T (= m_c > 0)$ is always positive scalar, hence it is also invertible. In this case, from (10) F_n can be expressed as

$$F_n = F_n(\boldsymbol{x}, \boldsymbol{\tau}, F_t), \tag{11}$$

or a more detailed form

$$\begin{aligned} F_n &= [(\frac{\partial C}{\partial \boldsymbol{q}})\boldsymbol{M}^{-1}(\frac{\partial C}{\partial \boldsymbol{q}})^T]^{-1} \parallel \frac{\partial C}{\partial \boldsymbol{r}} \parallel \\ &\{-[\frac{\partial}{\partial \boldsymbol{q}}(\frac{\partial C}{\partial \boldsymbol{q}})\dot{\boldsymbol{q}}]\dot{\boldsymbol{q}} + (\frac{\partial C}{\partial \boldsymbol{q}})\boldsymbol{M}^{-1}(\boldsymbol{H}(\boldsymbol{q}, \dot{\boldsymbol{q}}) + \boldsymbol{G}(\boldsymbol{q}) + \boldsymbol{J_r}^T F_t)\} \\ &-[(\frac{\partial C}{\partial \boldsymbol{q}})\boldsymbol{M}^{-1}(\frac{\partial C}{\partial \boldsymbol{q}})^T]^{-1} \parallel \frac{\partial C}{\partial \boldsymbol{r}} \parallel \{(\frac{\partial C}{\partial \boldsymbol{q}})\boldsymbol{M}^{-1}\}\boldsymbol{\tau} \\ &\triangleq a(\boldsymbol{x}_1, \boldsymbol{x}_2) + \boldsymbol{A}(\boldsymbol{x}_1)\boldsymbol{J}_r^T F_t - \boldsymbol{A}(\boldsymbol{x}_1)\boldsymbol{\tau}, \end{aligned} \tag{12}$$

where, $a(\boldsymbol{x}_1, \boldsymbol{x}_2)$ is a scalar representing the first term in the expression of F_n, and $\boldsymbol{A}(\boldsymbol{x}_1)$ is an l vector to represent the coefficient vector of $\boldsymbol{\tau}$ in the same expression. Equations (7) and (11) compose a constrained dynamical system that can be controlled.

Substituting the (12) into (6), the state equation of the system including the constrained force (as $F_n > 0$) can be rewritten as

$$\begin{aligned} \dot{\boldsymbol{x}}_1 &= \boldsymbol{x}_2, \\ \dot{\boldsymbol{x}}_2 &= -\boldsymbol{M}^{-1}[\boldsymbol{H}(\boldsymbol{x}_1, \boldsymbol{x}_2) + \boldsymbol{G}(\boldsymbol{x}_1) - \boldsymbol{J}_c^T(\boldsymbol{x}_1)a(\boldsymbol{x}_1, \boldsymbol{x}_2)] \\ &\quad +\boldsymbol{M}^{-1}[(\boldsymbol{I} - \boldsymbol{J}_c^T\boldsymbol{A})\boldsymbol{\tau} + (\boldsymbol{J}_c^T\boldsymbol{A} - \boldsymbol{I})\boldsymbol{J}_r^T F_t]. \end{aligned} \tag{13}$$

The model of the constrained dynamical system is depicted in Fig. 2. Note that the solution of these dynamic equations will always satisfy the constrained equation (4), so that the normal position error will always be zero. On the other hand, in these dynamic equations of constrained motions, the constrained force F_n is not included, but with the control law presented in the following section, the force can be controlled explicitly.

4 FORCE AND POSITION CONTROLLER

4.1 Controller using predicted constraint condition

Reviewing the dynamic equation (3) and constraint condition (4), it can be found that as $l > 1$, the number of input generalized forces is more than that of the constrained forces. From this point and (12) we can claim that there is some redundancy of constrained force between the input torque $\boldsymbol{\tau}$, and the constrained force F_n. This condition is much similar to the kinematical redundancy of redundant manipulator. Based on the above argument and assuming that, the parameters of the (12) are known and its state variables could be measured, and $a(\boldsymbol{x}_1, \boldsymbol{x}_2)$ and $\boldsymbol{A}(\boldsymbol{x}_1)$ could be calculated correctly, which means that the constraint condition $C = 0$ is prescribed. As a result, a control law is derived and can be expressed as

$$\begin{aligned} \boldsymbol{\tau} = -\boldsymbol{A}^+(\boldsymbol{x}_1)\Big\{ F_{nd} - a(\boldsymbol{x}_1, \boldsymbol{x}_2) - \boldsymbol{A}(\boldsymbol{x}_1)\boldsymbol{J}_R^T F_t \Big\} \\ +(\mathbf{I} - \boldsymbol{A}^+(\boldsymbol{x}_1)\boldsymbol{A}(\boldsymbol{x}_1))\boldsymbol{k}, \end{aligned} \tag{14}$$

where $\mathbf{I}$ is an identity matrix of $l \times l$, F_{nd} is the desired constrained forces, $\boldsymbol{A}(\boldsymbol{x}_1)$ is defined in (12) and $\boldsymbol{A}^+(\boldsymbol{x}_1)$ is a pseudoinverse matrix of it, $a(\boldsymbol{x}_1, \boldsymbol{x}_2)$ is also defined in (12). It can be confirmed easily that when the torque $\boldsymbol{\tau}$ calculated by Eqs.(14) be input to (12), we obtain $F_n = F_{nd}$. This means the fact that the transmitting process of realizing F_n by $\boldsymbol{\tau}$ is instantaneous, enables

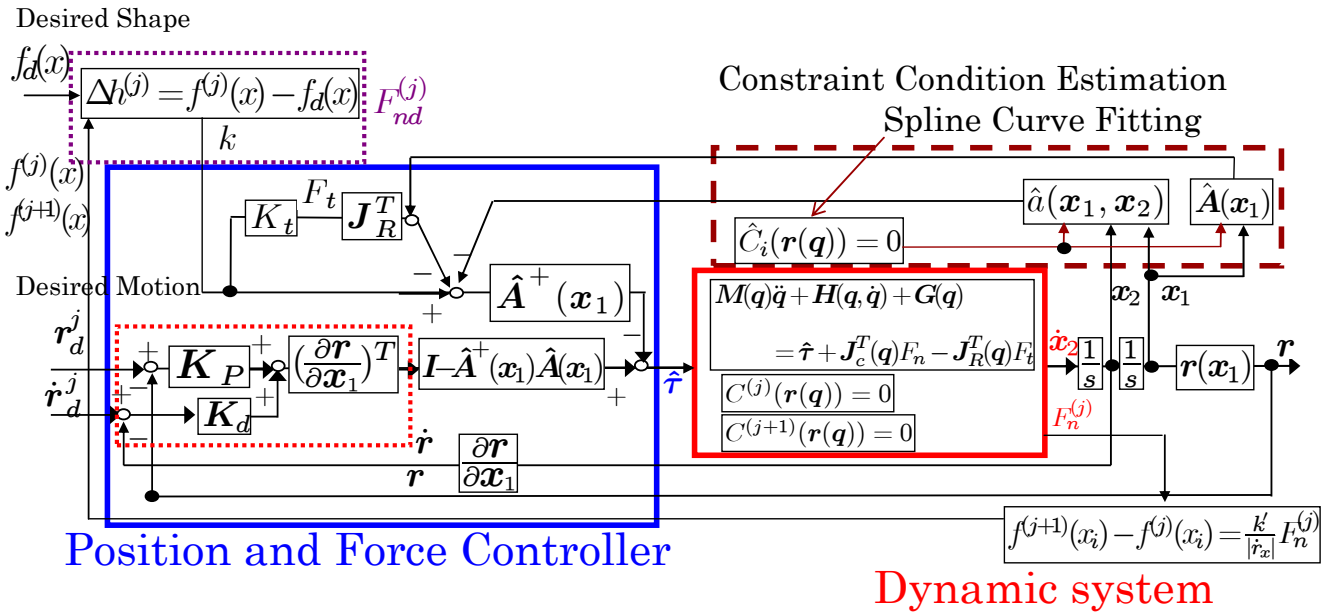

Fig. 3: Shape-grinding position / force control system

the proposed system to be invertible. $\boldsymbol{k}$ is an arbitrary vector which is defined as

$$\boldsymbol{k} = \tilde{\boldsymbol{J}}_r^T(\boldsymbol{q})\Big\{\boldsymbol{K}_p(\boldsymbol{r}_d - \boldsymbol{r}) + \boldsymbol{K}_d(\dot{\boldsymbol{r}}_d - \dot{\boldsymbol{r}})\Big\}, \tag{15}$$

where $\boldsymbol{K_p}$=$diag[k_{p1}, \cdots, k_{pl}]$ and $\boldsymbol{K_d}$=$diag[k_{d1}, \cdots, k_{dl}]$ are coefficient matrices applied to the position and the velocity control by the redundant degree of freedom of $\boldsymbol{A}(\boldsymbol{x}_1)$, $\boldsymbol{r}_d(\boldsymbol{q})$ is the desired position vector of the end-effector along the constrained surface and $\boldsymbol{r}(\boldsymbol{q})$ is the real position vector of it. The controller presented by (14) and (15) assumes that the constraint condition $C = 0$ be known precisely even though the grinding operation is a task to change the constraint condition. This looks like to be a contradiction, so we need to observe time-varying constraint conditions in real time by using grinding tip as a touch sensor.

The time-varying constraint condition is estimated as an approximate function by using position of the grinding tip. The estimated condition is denoted by $\hat{C} = 0$. Hence, $a(\boldsymbol{x}_1, \boldsymbol{x}_2)$ and $\boldsymbol{A}(\boldsymbol{x}_1)$ including $\partial\hat{C}/\partial\boldsymbol{q}$ and $\partial/\partial\boldsymbol{q}(\partial\hat{C}/\partial\boldsymbol{q})$ are changed to $\hat{a}(\boldsymbol{x}_1, \boldsymbol{x}_2)$ and $\hat{\boldsymbol{A}}(\boldsymbol{x}_1)$ as shown in (16), (17).

$$m_c{}^{-1}\| \frac{\partial\hat{C}}{\partial\boldsymbol{r}} \|\{-[\frac{\partial}{\partial\boldsymbol{q}}(\frac{\partial\hat{C}}{\partial\boldsymbol{q}})\dot{\boldsymbol{q}}]\dot{\boldsymbol{q}} + (\frac{\partial\hat{C}}{\partial\boldsymbol{q}})\boldsymbol{M}^{-1}(\boldsymbol{h}+\boldsymbol{g})\} \triangleq \hat{a}(\boldsymbol{x}_1, \boldsymbol{x}_2) \tag{16}$$

$$m_c{}^{-1}\| \frac{\partial\hat{C}}{\partial\boldsymbol{r}} \|\{(\frac{\partial\hat{C}}{\partial\boldsymbol{q}})\boldsymbol{M}^{-1}\} \triangleq \hat{\boldsymbol{A}}(\boldsymbol{x}_1) \tag{17}$$

As a result, a controller based on the estimated constrained condition is given as

$$\hat{\boldsymbol{\tau}} = -\hat{\boldsymbol{A}}^+(\boldsymbol{x}_1)\Big\{F_{nd} - \hat{a}(\boldsymbol{x}_1, \boldsymbol{x}_2) - \hat{\boldsymbol{A}}(\boldsymbol{x}_1)\boldsymbol{J}_R^T F_t\Big\} + (\mathbf{I} - \hat{\boldsymbol{A}}^+(\boldsymbol{x}_1)\hat{\boldsymbol{A}}(\boldsymbol{x}_1))\boldsymbol{k}, \tag{18}$$

Fig.3 illustrates a control system constructed according to the above control law that consists of a position feedback control loop and a force feedfoward control.

Experiments to control position and force of the grinder had shown that the maximal position error is 8[mm] and maximal force error is 3[N].

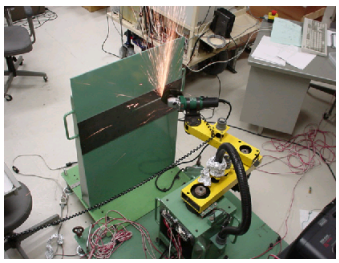

Fig. 4: The experiment when the constraint is known

4.2 Shape grinding

In the past, we did the experiment when working surface was flat(which is shown in Fig.4), so we can just do flat grinding. Now we want to grind the work-piece into the one with different kinds of shapes, for example, grinding the flat surface into a curved one, just like dipicted in Fig. 5. In Fig. 5, we can find that the desired working surface is prescribed, which means the desired constrained condition C_d can be given and known, so

$$C_d = y - f_d(x) = 0. \tag{19}$$

But the constrained condition $C^{(j)}$ (j=1, 2, $\cdots$) changed by repeating grinding that is in the box of Constraint Dynamical System in Fig. 3 is hard to be predefined. First of all assume $C^{(1)}$=0 is given. Provided $C^{(j)}$=0 is determined and if $C^{(j+1)}$=0 can be decided

through considering $F_n(t)$, $r(t)$, $\dot{r}(t)$, then the consecutive ground surfaces $C^{(1)}$=0, $C^{(2)}$=0, $\cdots$ can be defined continuously. First we assume j-th ground constraint condition as:

$$C^{(j)} = y - f^{(j)}(x) = 0 \tag{20}$$

where, y is the y position of manipulator's end-effector in the coordinates Σw depicted in Fig. 5. $f^{(j)}(x)$ is the working surface remained by j-th grinding. And $f^{(j)}(x)$ is a function passing through all points, $(x_1,\ f^{(j)}(x_1))$, $(x_2,\ f^{(j)}(x_2))$, $\cdots$, $(x_p,\ f^{(j)}(x_p))$, these observed points representing the j-th constraint condition obtained from the grinding tip position since we proposed previously the grinding tip is used for the touching sensor of ground new surface. Here we assume $f^{(j)}(x)$ could be represented by a polynomial of $(p-1)$-th order of x. Given the above p points, we can easily decide the parameters of polynomial function $y = f^{(j)}(x)$. If the current constrained condition can be got successfully, which means the current working surface $f^{(j)}(x)$ can be detected correctly, the distance from the current working surface to the desired working surface which is expressed as $\Delta h^{(j)}$ shown in Fig. 5 can be obtained easily,

$$\Delta h^{(j)}(x_i) = f^{(j)}(x)\big|_{x=x_i} - f_d(x)\big|_{x=x_i} \tag{21}$$

In this case, we can obviously find that the desired constrained force should not be a constant. It should be changed while $\Delta h^{(j)}$ changes. So we redefine the desired constrained force $F_{nd}^{(j)}$ as a function of $\Delta h^{(j)}$, shown as follows:

$$F_{nd}^{(j)}(x_i) = k\Delta h^{(j)}(x_i) \tag{22}$$

where, k is a constant.

$F_{nd}^{(j)}(x_i)$is given to the controller(18), then the exerted force $F_n^{(j)}(x_i)$ is determined by(12). New-ground surface $f^{(j+1)}(x_i)$ can be represented through exerted force $F_n^{(j)}(x_i)$ and previous constraint $f^{(j)}(x_i)$ as

$$f^{(j+1)}(x_i) - f^{(j)}(x_i) = \frac{k'}{|\dot{r_x}|} F_n^{(j)}(x_i) \tag{23}$$

where, k' is a constant, and grinding tip's velocity $|\dot{r_x}|$ is the real velocity of grinder, which is output from Constraint Dynamical system in Fig 3. Here is why we set the coefficient of $F_n^{(j)}(x_i)$ with both k' and $|\dot{r_x}|$. According to the fact of grinding process, we all know that with a same constrained force, the bigger grinder's velocity will cause thinner ground depth. Therefore, coefficient of $F_n^{(j)}(x_i)$ should be modeled as to be divided by velocity term $|\dot{r_x}|$.Then k' will be set along with $|\dot{r_x}|$ to make the influence of $F_n^{(j)}(x_i)$ more reasonable.

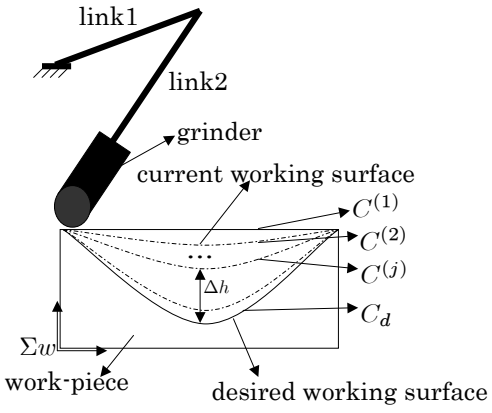

Fig. 5: The model of shape grinding

A condition that the new object shape $f^{(j+1)}(x_i)$ have to satisfy, i.e.,

$$y = f^{(j+1)}(x_i) \tag{24}$$

Then $C^{(j+1)}$ can also be known:

$$C^{(j+1)} = y - f^{(j+1)}(x) = 0 \tag{25}$$

So, starting from $C^{(1)}$, all of $C^{(j)}$ can be decided. What we want to emphasize is C_i represents the resulted ground shape of the object defined in the shape-grinding simulator. In the next part, we will introduce several estimation methods which are used to get $\hat{C}_i$ in current time.

4.3 Constraint condition description

The j-th constrained surface $C^{(j)}$=0, meaning j-th grinding procedure, defined in the previous section is a result of grinding, but the grinding controller have to assume that $C^{(j)}$=0 is unknown since the shape of $C^{(j)}$=0 is the result of grinding remained on the work object in nature. Therefore we need an estimator of $C^{(j)}$=0 while the grinding process proceeding. On this section we compare three methods to estimate grinding surface in real time such as linear function, quadratic function, and spline curve. Three simulations have been done based on different constraint conditions. Here, an unknown constrained condition is estimated as following,

(Assumptions)

1. The end point position of the manipulator during performing the grinding task can be surely measured and updated.
2. The grinding task is defined in $x-y$ plane.
3. When beginning to work, the initial condition of the end-effector is known and it has touched the work object.
4. The chipped and changed constraint condition can be approximated by connections of minute sections.

Three methods which are fitting by linear function, quadratic function and spline function had been used to get the online estimation of the unknown constrained condition.

4.3.1 Fitting by linear function

The unknown constrained surface is fitted by line equation and is expressed as,

$$\hat{C}_{i+1}^{(j)} = y - \alpha x - \beta, \tag{26}$$

where $\hat{C}_{i+1}^{(j)} = \hat{C}^{(j)}((i+1)\Delta t)$ and $\Delta t = 0.0007[s]$ is control period.

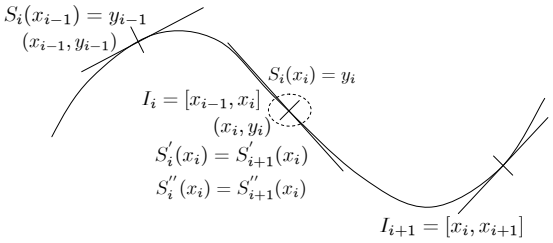

Fig. 6: Fitting by cubic spline curve

The end-effector position at time $(i-1)\Delta t$ and $i\Delta t$ are denoted respectively as (x_{i-1}, y_{i-1}), (x_i, y_i). As you know, a line $f(x) = \alpha x + \beta$ can be difined uniquely by two points,with this two points coefficients of the line equation α, β can be calculated. What we want to emphasize here is the predicted condition $\hat{C}_{i+1}^{(j)} = 0$ at time $t = (i+1)\Delta t$ is calculated on-line from current and past hand position of (x_{i-1}, y_{i-1}) and (x_i, y_i), and the estimation is not done based on the previous grinding result of $\hat{C}^{(j)} = 0$. So the proposed grinding method can be adopted to unknown target object's shape without prior knowledge.

Then the constrained conditional expression can be updated step by step.

4.3.2 Fitting by quadratic function

The unknown constrained surface is estimated by quadratic curve and is expressed as,

$$\hat{C}_{i+1} = y - (ax^2 + bx + c) \tag{27}$$

The end-effector position at time $(i-2)\Delta t$,$(i-1)\Delta t$, $i\Delta t$ are denoted respectively as(x_{i-2}, y_{i-2}), (x_{i-1}, y_{i-1}), and (x_i, y_i). Based on the three points,the coefficients of quadratic curve $(f(x) = ax^2 + bx + c)$ obviously can be calculated.

4.3.3 Fitting by cubic spline curve

The unknown constrained condition, which is in Fig. 3, is estimated and expressed as,

$$\hat{C}_{i+1} = y - [A_i(x - x_{i-1})^3 + B_i(x - x_{i-1})^2 + C_i(x - x_{i-1}) + D_i] \tag{28}$$

The end-effector position at time $(i-1)\Delta t$, $i\Delta t$ are denoted respectively as (x_{i-1}, y_{i-1}), (x_i, y_i).

The cubic spline curve denoted as

$$S_i(x) = A_i(x - x_{i-1})^3 + B_i(x - x_{i-1})^2 + C_i(x - x_{i-1}) + D_i, x \in [x_{i-1}, x_i](i = 1, 2, 3 \cdots n) \tag{29}$$

The constrained condition $\hat{C}_{i+1} = y - (A_i(x - x_{i-1})^3 + B_i(x - x_{i-1})^2 + C_i(x - x_{i-1}) + D_i)$ can be determined as follows.

Firstly, let $S_i(x)$ satisfy the following conditions shown in Fig. 6.

(A)Go through two ends of the interval

$$y_{i-1} = S_i(x_{i-1}) \tag{30}$$

$$y_i = S_i(x_i) \tag{31}$$

(B)First-order differential of the spline polynomials are equal at the end-point of adjoined function.

$$S_{i+1}'(x_i) = S_i'(x_i) \tag{32}$$

(C)Second-order differential of the spline polynomials are equal at the end-point of adjoined function.

$$S_{i+1}''(x_i) = S_i''(x_i) \tag{33}$$

Inputting (29) into (30), (31), (32) and (33), we can obtain:

$$D_i = y_{i-1}, (i = 1, 2, \cdots, n) \tag{34}$$

$$B_{i+1} = \frac{3(u_i - C_i)}{h_i} - 2B_i, (i = 1, 2, \cdots, n-1) \tag{35}$$

$$C_{i+1} = 3u_i - B_i h_i - 2C_i, (i = 1, 2, \cdots, n-1) \tag{36}$$

$$A_i = \frac{u_i - C_i}{h_i^2} - \frac{B_i}{h_i}, (i = 1, 2, \cdots, n) \tag{37}$$

Where, $h_i = x_i - x_{i-1}$, $u_i = (y_i - y_{i-1})/h_i$. From the above-mentioned result, the constrained conditional expression $\hat{\boldsymbol{C}}_{i+1}$ can be updated step by step.

Here, we can see that the spline curve is defined by two points and derivative at one point. Compared to the quadratic function fitting and linear function fitting, Fitting by cubic spline curve is more precise because derivative is used at the current hand position.

5 EXPERIMENT

The experiment when constraint surface is being estimated by quadratic spline curve method has been done successfully. Parameters of the grinding robot manipulator used in the experiment are: length of link 1 is 0.3[m], length of link 2 is 0.5[m], and the mass of link 1 is 12.28[kg], the mass of link 2 is 7.64[kg]. The specifications of first and second joints are as follows, the first joint: *AC* Servo Motor, 200V, 400W, 2.6A; the second joint: *AC* Servo Motor, 200V, 200W, 2.0A; both are made by YASKAWA ELECTRIC Co.. The desired constrained force, $F_{nd} = 10$[N], grinding resistance, $F_t = 0$[N]. Here the force control performance that the exerting force F_n be equal to the desired one, F_{nd}, is expected to be realized by compensating the effect generated by friction force F_t in (18). We had confirmed this force control accuracy improvement by real grinding experiments, so we will not discuss the influence of F_t in this paper, thus setting $F_t = 0$[N].

The desired constrained surface is denoted as

$$f(x) = 0.51 \tag{38}$$

The known constraint condition $C = y - 0.51$ has been recorded in Fig.7, at the same time, unknown constraint condition $\hat{C}$ which was estimated by cubic spline curve

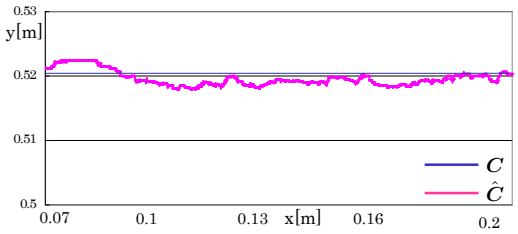

Fig. 7: Trajectory comparison of end effector between the known one and estimated one

fitting method through (28), has also been recorded in Fig.7(in Fig.7, part $0.00m$ to $0.07m$ along $x-axis$,in other words, part $0.0s$ to $2.4s$ in time span, has been cut since during this interval, a big crash happened between manipulator hand and work piece, moreover this same treatment has been done to all the experiment results). From this comparison figure, we can find that using the proposed estimation method, the shape of constraint surface can be estimated very well. And we consider this kind of coincidence has provided an initial proof for the operability of this proposed controlling method.

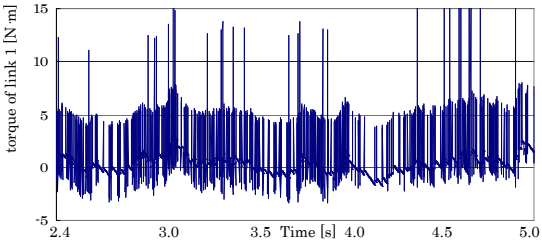

Fig. 8: Change of τ_1

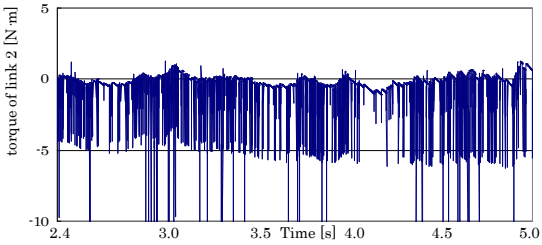

Fig. 9: Change of τ_2

Then let's take a look at the torque experiment results through Fig.8 to Fig.11. τ_1 and τ_2 which had been calculated by (14) are shown in Fig.8 and Fig.9, $\hat{\tau}_1$ and $\hat{\tau}_2$ which had been calculated by (18) are shown in Fig.10 and Fig.11. $\tau_i(i=1,2)$ and $\hat{\tau}_i(i=1,2)$ are different from each other, as we discussed in 4.1. When $\tau_i(i=1,2)$ being calculated , the already known constraint condition $C=0$ is used, but when $\hat{\tau}_i(i=1,2)$ being calculated, the estimated constraint condition $\hat{C}=0$ is used, which means that $\hat{\tau}_i(i=1,2)$ is the calculation result from the estimation of constraint surface using cubic spline curve fitting method.

Here we notice that torque is oscillating no matter under the situation of known constraint condition $C=0$ (Fig.8 and Fig.9) or the situation of estimated constraint condition $\hat{C}=0$(Fig.10 and Fig.11), so obviously the oscillation does not just come from the estimated constraint condition. Therefore, we pay attention on

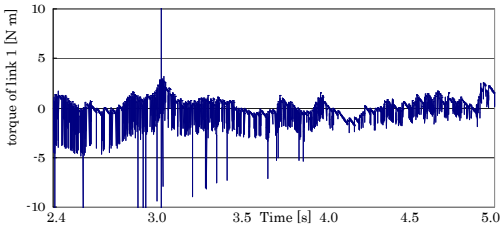

Fig. 10: Change of $\hat{\tau}_1$

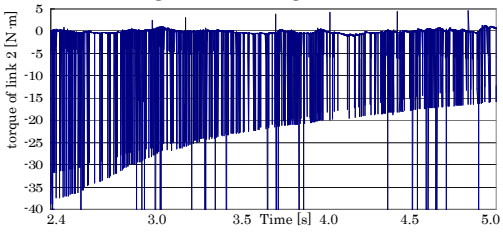

Fig. 11: Change of $\hat{\tau}_2$

the reason why torque is oscillating under the situation of known constraint condition ($C=0$) at first. A lot of investigation has been done, we found the oscillation occurred when constraint condition is known ($C=0$), totally comes from the oscillation of the two angle velocity $\dot{\boldsymbol{q}}_m(m=1,2)$, as shown in Fig.12, $\dot{\boldsymbol{q}}_m(m=1,2)$ is oscillating through the entire experiment time ($5s$), and the influence has been brought into the change of torque shown in Fig.8 and Fig.9. This kind of oscillation is not to be wanted as the torque should be steady to drive the grinding robot. Therefore, we processed the angle velocity of each link $\dot{\boldsymbol{q}}_m(m=1,2)$ by moving average method (Eqn.39) to eliminate the oscillation.

$$\dot{\boldsymbol{q}}(i\Delta t)=\frac{1}{n}(\sum_{j=i-n}^{i}\dot{\boldsymbol{q}}(i\Delta t)) \qquad (\Delta t=0.7ms) \qquad (39)$$

After some trial experiment when n is set as $n=2,3,4,5,10,15,20,25,30$, we find when $n=30$, the torque's oscillation can be weaken to steady state. The processed $\dot{\boldsymbol{q}}_m(m=1,2)$ is shown in Fig.13.

With this processed angle velocity $\dot{\boldsymbol{q}}_m(m=1,2)$, the torque's change is shown in Fig.14 and Fig.15. From Fig.14 and Fig.15, we can find that torque's oscillation has been eliminated. Although the change of torque is still out of flatness, but since the period of torque's jump now is more or less $210ms$, which is much bigger than the period of angle velocity's jump($\Delta t=0.7ms$), we can declare that the influence of oscillation from angle velocity's jump has been totally eliminated when torque $\tau_i(i=1,2)$ is calculated.

6 CONCLUSIONS

The presented methodology allows computation of the forces, as an alternative to sensing. Hence, the system is controlled with no force sensor, instead of that, requiring measurement of changing constraint condition. The cubic spline curve fitting for changing and unknown constraint surface which is due result of grinding nature, is used in the shape-grinding experiment.

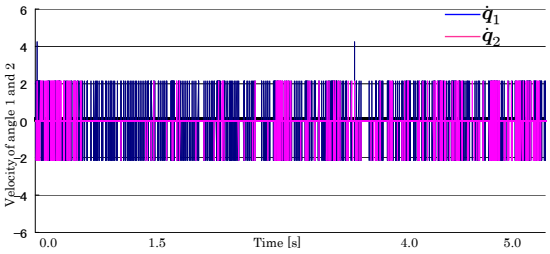

Fig. 12: Change of two angle velocity

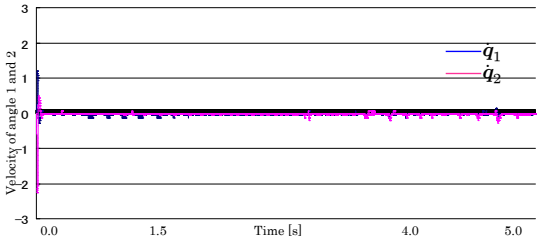

Fig. 13: Change of two angle velocity

Until now, we have done the grinding experiment when constraint surface is flat by this proposed controlling method without any force sensor. But there are still some unfavorable experiment phenomenon appeared in torque's change such as the oscillation we discussed in former chapter. Next we will try to do the grinding experiment by using the angle velocity which is processed by moving average method with cubic spline-estimate constraint condition.

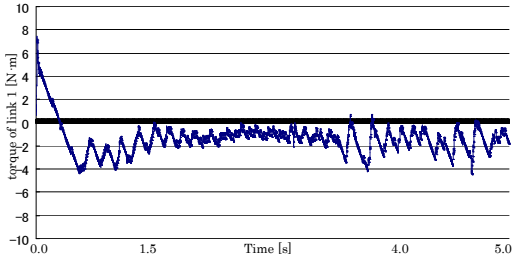

Fig. 14: Change of τ_1 by using the processed angle velocity

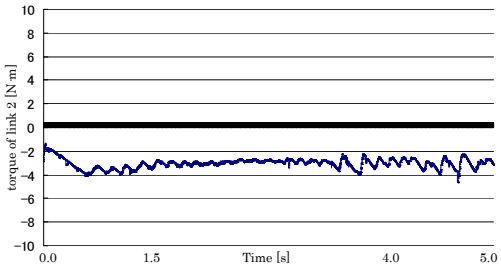

Fig. 15: Change of τ_2 by using the processed angle velocity

参考文献

[1] M.H.Raibert and J.J.Craig: Hybrid Position/Force Control of Manipulators, Trans. of the ASME, J. of Dynamic Systems, Measurement and Control, Vol.102, pp.126-133, June, 1981.

[2] James K. Mills and Andrew A. Goldenberg: Force and Position Control of Manipulators During Constrained Motion Tasks, IEEE Trans. on Robotics and Automation, Vol.5, No.1, pp.30-46, Feb., 1989.

[3] S. Arimoto: Mechanics and Control of Robot(in Japanese), Asakura Publishing Co., Ltd., Tokyo, Japan, 1990.

[4] Mamoru Minami and Weiwei Xu: Shape-grinding by Direct Position / Force Control with Online Constraint Estimation, IEEE, Conference IROS2008, Nice, France, 2008.

[5] T. Yoshikawa: Dynamic Hybrid Position/Force control of Robot Manipulators — Description of Hand Constraints and Calculation of Joint Driving Force, IEEE J. on Robotics and Automation, Vol.RA-3, No.5, pp.386-392, 1987.

[6] L. Whitcomb, S. Arimoto, T. Naniwa and F. Osaki: Experiments in Adaptive Model-Based Force Control, IEEE Control Systems Society, Vol.16, No.1, pp.49-57, 1996.

[7] S. Arimoto: Joint-Space Orthogonalization and Passivity for Physical Interpretations of Dextrous Robot Motions under Geometric Constrains, Int. J. of Robust and Nonlinear Control, Vol.5, pp.269-284, 1995.

[8] T. Naniwa and S. Arimoto: Model-Based Adaptive Control for Geometrically Constrained Robot Manipulators, Trans. of Institute of Systems, Control and Information Engineers, Vol.8, No.9, pp.482-490, 1995.

[9] D.Wang and N.H. McClamroch: Position and Force Control for Constrained Manipulator Motion: Lyapunov's Direct Approach, IEEE Trans. Robotics and Automation, Vol.9, pp.308-313, 1993.

[10] Z. X. Peng and N. Adachi: Position and Force Control of Manipulators without Using Force Sensors(in Japanese), Trans. of JSME(C), Vol.57, No.537, pp.1625-1630, 1991.

[11] T. Yoshikawa, T. Sugie and M. Tanaka: Dynamic Hybrid Position/Force control of Robot Manipulators - Controller Design and Experiment-, IEEE J. on Robotics and Automation, Vol.RA-4, No.6, pp.699-705, 1988.